

CrystEngComm

Accepted Manuscript



This is an *Accepted Manuscript*, which has been through the Royal Society of Chemistry peer review process and has been accepted for publication.

Accepted Manuscripts are published online shortly after acceptance, before technical editing, formatting and proof reading. Using this free service, authors can make their results available to the community, in citable form, before we publish the edited article. We will replace this *Accepted Manuscript* with the edited and formatted *Advance Article* as soon as it is available.

You can find more information about *Accepted Manuscripts* in the [Information for Authors](#).

Please note that technical editing may introduce minor changes to the text and/or graphics, which may alter content. The journal's standard [Terms & Conditions](#) and the [Ethical guidelines](#) still apply. In no event shall the Royal Society of Chemistry be held responsible for any errors or omissions in this *Accepted Manuscript* or any consequences arising from the use of any information it contains.

Cite this: DOI: 10.1039/c0xx00000x

www.rsc.org/crystengcomm

ARTICLE

Investigating the Dissolution of the Metastable Triclinic Polymorph of Carbamazepine using *in situ* Microscopy

M. O'Mahony,^{a,b} C. C. Seaton,^a D.M. Croker,^a S.Veesler,^c Å. C. Rasmuson^a and B. K. Hodnett^a

Received (in XXX, XXX) Xth XXXXXXXXX 20XX, Accepted Xth XXXXXXXXX 20XX

DOI: 10.1039/b000000x

Despite a tendency to undergo solution-mediated polymorphic transformation, the dissolution behaviour of the metastable FI (triclinic) polymorph of the pharmaceutical compound carbamazepine (CBZ) was investigated using *in situ* optical microscopy. Experiments were performed at an undersaturation where single crystals of the metastable FI polymorph dissolved. Dissolution in different solvents was investigated at a constant undersaturation. Separately the sublimation of FI was examined and additionally the dissolution was observed at undersaturations where the more stable FIII polymorph crystallized. The results show that both the dissolution and sublimation of FI occur primarily in the direction of the *a*-axis of the FI crystal structure where the CBZ molecules are found to stack in this direction. The order for the dissolution rate of FI was acetonitrile \geq methanol $>$ ethanol. The order of the dissolution rates in each of the solvents is inversely correlated to the viscosity and the binding energy of the solvents with the (100) surface of FI in each of the solvents. This suggests that the rate determining step for the dissolution may be either the diffusion or the detachment of CBZ molecules from the surface of FI. A notable difference in dissolution behaviour is also observed at undersaturations where the more stable FIII polymorph nucleates and grows.

Introduction

The dissolution of crystalline material lies at the heart of a variety of natural and synthetic processes, such as mineral replacement reactions in the earth's crust and the production of fine chemicals.^{1,2,3} Studies have shown that crystal growth mechanics can also be used to explain the dissolution of crystalline phases - highlighting the reciprocity between crystal growth and dissolution mechanisms.⁴ Changes to crystal morphology during dissolution and growth in the presence of specific additives are well-understood to occur through the stereoselective binding of such additives at specific crystal faces.⁵⁻¹⁰ In the case of a metastable crystal phase, the role of different solvents to affect dissolution has not yet been studied in detail.

Dissolution can be modelled as the diffusion of solute molecules across a boundary layer from the surface of the solid into the bulk solution, where the difference between the bulk solution concentration and the solubility of the solid provides the driving force for dissolution.¹¹ Dissolution rates measured with this model are used as a prognostic tool for oral drug absorption and bioavailability of crystalline active pharmaceutical ingredients (APIs).^{12,13} It is well known that APIs can often form more than one crystal structure or polymorph. This is of particular relevance in the manufacture of APIs because different polymorphs exhibit different physicochemical properties such as solubility, melting point, dissolution rate, etc.¹⁴ In the case where a metastable polymorph has crystallized from solution and

continues to interact with a bulk solution phase the possibility exists for a metastable polymorph to dissolve and a more stable polymorph to nucleate and grow – a process known as solution-mediated polymorphic transformation (SMPT). Dissolution of the metastable phase plays a vital role in the process of SMPT³ and so understanding the dissolution behaviour of metastable phases is important to develop a deeper understanding of the SMPT process. Such understanding may be subsequently used to further control the manufacture of fine chemicals such as APIs. The dissolution conditions experienced by the metastable phase during SMPT, can be understood by analysing the solution concentration with time.³ If growth of the stable phase is relatively slow compared to dissolution of the metastable phase, the metastable phase will typically dissolve, under conditions of low driving force. Conversely, if the stable phase growth is rapid relative to the dissolution of the metastable phase, the metastable phase is expected to dissolve under conditions of higher driving force. Different solvents may also affect the dissolution rate of a metastable polymorph and potentially impact the kinetics of the SMPT. The metastable FI polymorph of the pharmaceutical compound carbamazepine (CBZ) has a strong tendency to transform to the stable FIII polymorph via SMPT.¹⁵ Herein we use *in situ* optical microscopy to study the dissolution behaviour of the metastable FI polymorph in different solvents at high driving force for the dissolution and separately, at low driving force for the dissolution (where transformation to FIII is possible).

Experimental

FI Polymorph Preparation and Solubility

Pharmaceutical grade carbamazepine (FIII) was obtained from POLPHARMA S.A. (Starogard Gdański, Poland) and stored in the presence of silica gel (0% humidity). ACS reagent grade ethanol (EtOH), methanol (MeOH) and acetonitrile (MeCN) were used having a purity of 99.9%, ≥99.8 % and 99.9%, respectively.

Single crystals of the FI CBZ polymorph were prepared by heating FIII CBZ powder under a glass cover in the oven at 170°C for 2.5 hrs. under full vacuum. Needle-like particles were grown on the underside of the glass cover by sublimation with approx. dimensions: 2mm in length, 0.1mm in width and 0.05 mm depth. Single crystal X-ray diffraction (Oxford Diffraction Xcalibur system) was used to identify the needle-like particles as the triclinic FI polymorph of carbamazepine. These single crystals were used to investigate the dissolution behaviour of FI and examine the effect of solvent on the dissolution rate of FI.

The solubility of FIII was measured in acetonitrile. Excess FIII was added to approximately 30 mL of acetonitrile in a sealed test tube. The test tube was then placed in a thermostatic water bath (Grant GR150, S38 stainless steel, ±0.02 °C) and agitation was provided with the use of a PTFE-coated magnetic stirrer bar in the test tube. FIII and acetonitrile were allowed to equilibrate for 24 hrs. at each temperature and afterwards the suspended solid was allowed to settle for ~30 min. A solution sample was carefully filtered into a preweighed vial and weighed to determine the solution mass. After drying, the remaining solute was weighed and the concentration was expressed as g CBZ /g solvent. The excess solid was sampled at the time of sampling the solution and analysed by powder X-ray diffraction to ensure that no transformation of FIII occurred in the excess solid phase. During each solubility measurement the temperature was observed to be accurate to within ±0.05 °C.

Dissolution Studies

The dissolution rate of the FI polymorph was investigated using in situ optical microscopy under conditions of constant undersaturation. Undersaturation is defined by

$$\sigma_u = 1 - \left(\frac{C}{C^*} \right)$$

where C and C^* are solution concentration and solubility, respectively. A low undersaturation value is a concentration which is close to the solubility of the metastable FI polymorph and a higher undersaturation value is further from the solubility of FI. Thus, in conditions of low undersaturation with respect to the FI polymorph, the solution is much more supersaturated with respect to the stable FIII polymorph of CBZ by comparison to conditions where the solution is highly undersaturated with respect to FI.

All dissolution experiments were performed within a microscope holding cell, used to hold and seal a quiescent solution sample and single crystal of FI – approx. dimensions: 2mm in length, 0.1mm in width and 0.05 mm depth. This setup (Anacrismat) has been previously used to investigate solution

mediated phase transformations of a pharmaceutical compound¹⁶ and a protein¹⁷. The microscope holding cell was designed to fit within an adapted Peltier unit which facilitated temperature control of the cell (±0.1 °C). The contents of the cell were viewed using an inverted microscope at magnification 40x. In order to achieve solution concentrations with a known level of undersaturation specific masses of CBZ and solvent were weighed out to an approximate volume of 2 mL in the microscope holding cell and then sealed to prevent any loss of solvent. The contents of the cell were heated until complete dissolution was achieved. The clear solution was then cooled to the experimental temperature before addition of a single FI crystal. The dissolution of FI was followed by time lapsed imaging of the single crystal in solution using automated software. Where only the dissolution of FI occurred in the cell the dissolution rate was measured by monitoring the length of the FI needle-like crystal over time. The mass of the FI single crystal (<10 µg) of CBZ was negligible by comparison to the mass of CBZ already in solution and thus it can be assumed that the undersaturation remained constant during the dissolution experiments (except in cases where FIII crystallized in solutions having low undersaturation with respect to FI CBZ).

The dissolution rate of FI was measured in each solvent and at the different temperatures where the undersaturation was set to $\sigma_u = 0.18$. This was found to be the optimum concentration to study only the dissolution of FI avoiding the nucleation of the stable FIII polymorph. The dissolution of FI in conditions of lower undersaturation ($\sigma_u = 0.045$, higher supersaturation with respect to FIII) was also examined in ethanol. Separately, the sublimation of FI was measured using a hot stage (Linkam controller, ±0.1 °C) in conjunction with a Zeiss A1m imager microscope. Time lapsed images of the sublimation were captured using automated software.

Computational Modelling

Molecular interactions were investigated between solvent molecules using the (100) surface of FI. The binding energy was calculated using the force field of No et al.¹⁸ with atomic charges generated from ab initio calculations. The geometry of each molecule was initially optimised by DFT calculations in orca (PBE-D3/TZVP)¹⁹ and atomic charges calculated by fitting to the electrostatic potential. The position and orientation of the solvent molecules were optimised using the differential evolution (DE)²⁰ global optimisation algorithm (control parameters: K, F, Gmax, Np = 0.9, 0.8, 2000, 60). Solvent molecules (1 to 6) were optimised onto a constructed (100) surface of the FI polymorph (8 molecules) where the positions of the surface molecules were held fixed during the optimisation. The optimisation was undertaken by sequential addition of solvent molecules, thus one molecule was optimised and then held in roughly that position while the second molecule was optimised and so on. The binding interaction was normalised by the total number of molecules in the calculation. Position and orientation of the additional solvent molecules are bound within the range $-20 \leq b, c \leq 20$ Å, $0 \leq a \leq 20$ Å, $0^\circ \leq \theta, \varphi, \gamma \leq 360^\circ$, while previously located solvent molecules were bound to be ±2 Å and ±45° around their existing values.

Results

FI Characterisation and Solubility

The single crystals grown by sublimation were analysed by single crystal XRD at room temperature and identified as having a triclinic unit cell with lattice parameters: $a = 5.2728(6)$, $b = 20.6510(3)$, $c = 22.3094(1)$ Å, $\alpha = 84.22(6)^\circ$, $\beta = 87.78(1)^\circ$ and $\gamma = 84.93(6)^\circ$. This confirmed the particles as single crystals of the FI polymorph of CBZ.²¹ Crystallographic faces of the FI needle-like crystals were also indexed (Fig. 1). The anisotropic FI crystals were shown to have dominant growth in the a lattice direction. The indexed (010) face was slightly larger in width than the (001) face. Conclusive indexing of the faces at the ends of the FI crystal was not possible due to their small size.

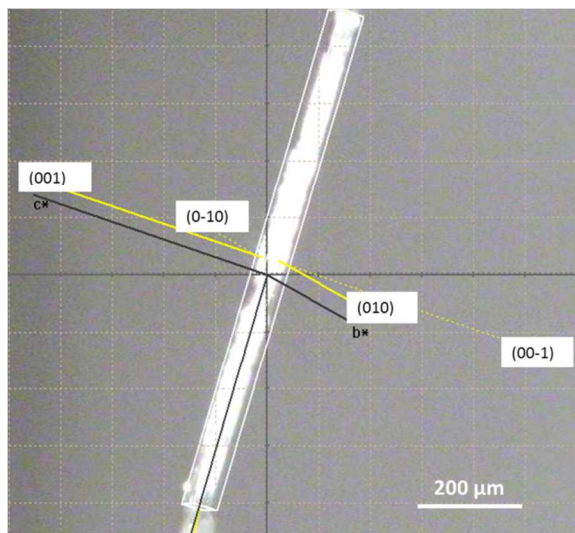


Fig. 1 The FI polymorph of CBZ indexed showing the dominant growth of the needle-like crystal along the length in the a lattice direction.

The solubility of FIII in acetonitrile measured for this work is presented in Table 1. Powder X-ray diffraction was used to identify that the solid phase in equilibrium with the solution was the stable FIII phase and that no solvates had formed. Recently, the solubility of stable FIII polymorph was also measured gravimetrically in methanol.²² In that same study, the solubility of FI was measured at 10, 22 and 30 °C in methanol using an in situ microscopy method.²² The polymorph solubility ratio can be considered independent of solvent assuming the solution activity coefficient, γ , in each solvent is independent of concentration,²³ which is likely for small differences in concentration and for a compound with relatively low solubility. The solubility of FIII in ethanol was also previously measured²² and using the measured polymorph solubility ratio, FI/FIII in methanol (mole fraction) the solubility of FI in ethanol and acetonitrile were calculated. The polymorph solubility ratio FI/FIII is 1.486, 1.362 and 1.309 at 10, 22 and 30 °C, respectively. The polymorph solubility ratio is 1.385 at 20 °C – the temperature at which the dissolution experiments were performed. The calculated FI solubility in ethanol was subsequently experimentally verified using the in situ

microscopy method.²² As there is an even smaller difference in solubility going from methanol to acetonitrile compared to the difference in going from methanol to ethanol (therefore, presumably less of an effect on the activity coefficient), it was assumed that the calculated solubility of FI in acetonitrile is close to the experimental value. The solubility of FI in each of the solvents is presented in Figure 2. The data show, as expected that the solubility increases with temperature and the order of the solubility in the solvents is MeOH>MeCN>EtOH.

Table 1 The solubility of FIII CBZ measured in acetonitrile and converted to mole fraction, x , used to calculate the solubility of FI - standard deviations are also included, $n = 3$.

T (°C)	Solubility FIII (g CBZ / g MeCN)	Mole fraction solubility FIII ($\times 10^3$)
5.0	0.0283 (± 0.0001)	4.89 (± 0.0174)
10.0	0.0329 (± 0.0003)	5.68 (± 0.0521)
15.0	0.0384 (± 0.0001)	6.63 (± 0.0174)
20.0	0.0452 (± 0.0001)	7.80 (± 0.0174)
25.0	0.0528 (± 0.0001)	9.10 (± 0.0174)
30.0	0.0609 (± 0.0001)	10.5 (± 0.0174)
35.0	0.0711 (± 0.0010)	12.2 (± 0.1740)

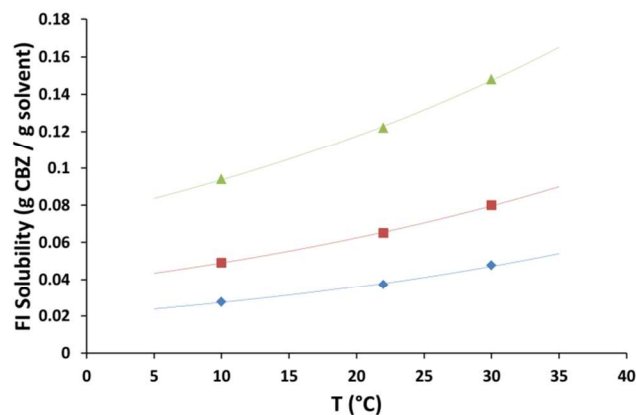


Fig. 2 FI solubility in methanol (MeOH) \blacktriangle and the calculated solubility of FI in ethanol (EtOH) \blacklozenge and acetonitrile (MeCN) \blacksquare using the solubility ratio of FI to FIII measured in methanol.²² The data are fitted with exponential functions.

Dissolution Experiments

Dissolution experiments were performed in ethanol at 20 °C and with $\sigma_u = 0.18$. In these conditions, dissolution of FI was observed without the crystallization of FIII (i.e. within the metastable zone width of FIII avoiding FIII nucleation). The dissolution of FI occurred in the a direction of the needle-like FI crystal such that the dissolution forced a rapid decrease in the crystallographic a lattice length of the FI crystal (Fig. 1). Notably the decrease in the length was faster than in the width (Fig. 3). Measurements were made with a resolution of approx. 10 μm .

The images for such a dissolution are shown in Fig. 3a-c and

related data shown in Fig. 3d. The example shows dissolution of FI in the *a* lattice direction was almost linear over time with a dissolution rate of $24 \mu\text{m}\cdot\text{min}^{-1}$. In contrast, the dissolution of FI in the width was approx. $1 \mu\text{m}\cdot\text{min}^{-1}$. The dissolution rate measurement in the *a* lattice direction was repeated for three similar sized crystals and this gave an average dissolution rate of $27 \mu\text{m}\cdot\text{min}^{-1} \pm 5 \mu\text{m}\cdot\text{min}^{-1}$.

The sublimation of FI was investigated at 145°C . The results are shown in Fig. 3e-h. The sublimation of FI occurred over a longer time frame by comparison to the dissolution. However, the results

show that the sublimation of FI also occurred primarily in the *a* lattice direction of the FI crystal similar to the dissolution. This was consistently observed in repeat experiments for both dissolution and sublimation. From the data in Fig. 3e, approximating the sublimation rate as linear and constant, the sublimation in the length of the FI was $\sim 2 \mu\text{m}\cdot\text{min}^{-1}$ whereas the width sublimed at $\sim 0.1 \mu\text{m}\cdot\text{min}^{-1}$.

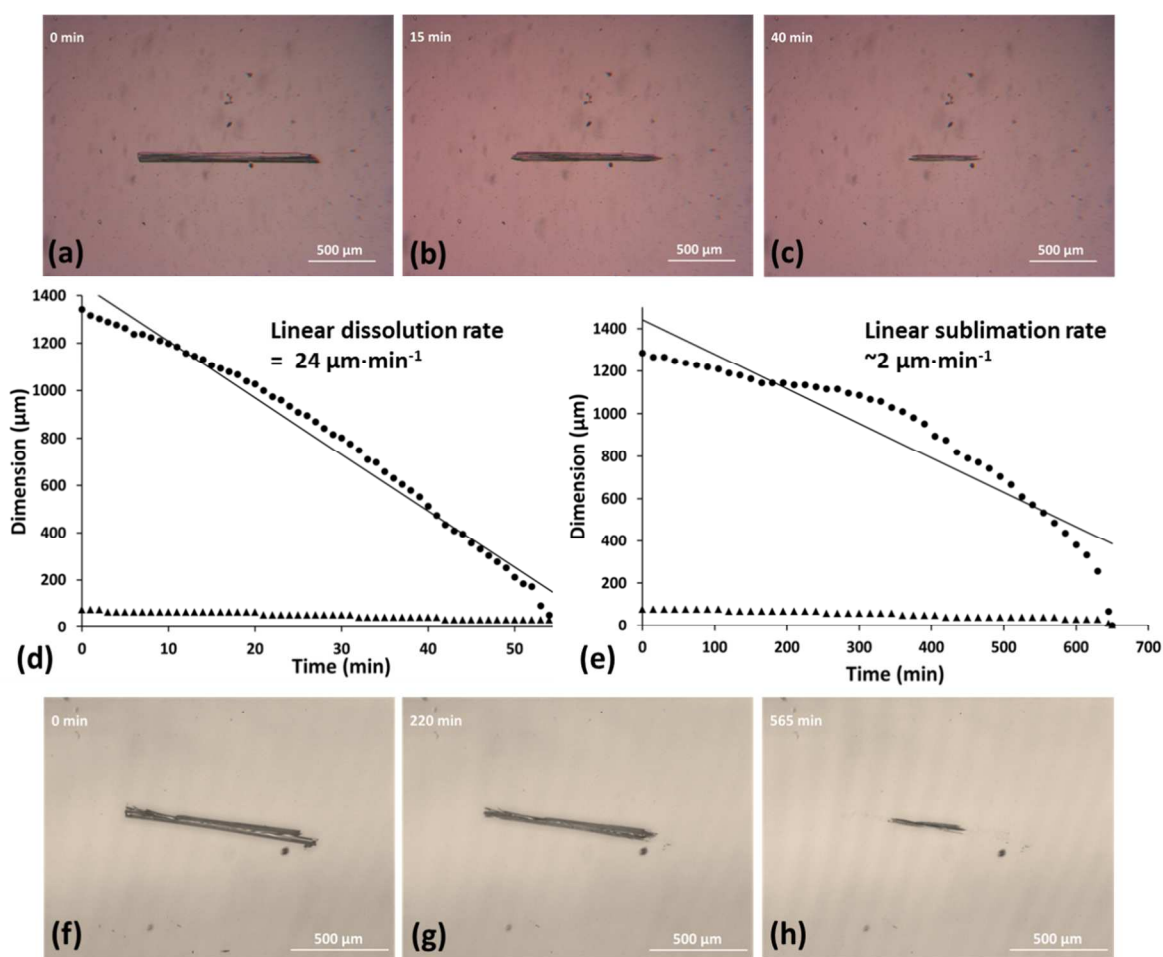


Fig. 3 *In situ* optical microscopy measurements. Dissolution: (a)-(c) time lapsed images showing the dissolution of FI in ethanol at 20°C with $\sigma_u = 0.18$ (solution concentration $0.0295 \text{ g CBZ} / \text{g EtOH}$). (d) dissolution measurement of the width \blacktriangle and length \bullet of the dissolving FI crystal over time. Sublimation: (e) Sublimation measurements of the width \blacktriangle and length \bullet of the subliming FI crystal from over time at 145°C . (f)-(h) Time lapsed images under the hot stage microscope showing the FI crystal subliming at 145°C .

The dissolution of FI in the *a* lattice direction was also observed in the solvents acetonitrile and methanol (see electronic supplementary information). This enable measurement of the dissolution rate in methanol and acetonitrile at the same constant $\sigma_u = 0.18$ at 20°C . The results are presented in Fig. 4a where the

average dissolution rate in each of the solvents is plotted against the solubility of FI in each solvent. The results show that the order of the dissolution rate is $\text{MeCN} \geq \text{MeOH} > \text{EtOH}$. While EtOH has the lowest solubility and lowest dissolution rate, the increasing order of the dissolution rates for MeCN and MeOH presented in Fig. 4a does not correlate with solubility.

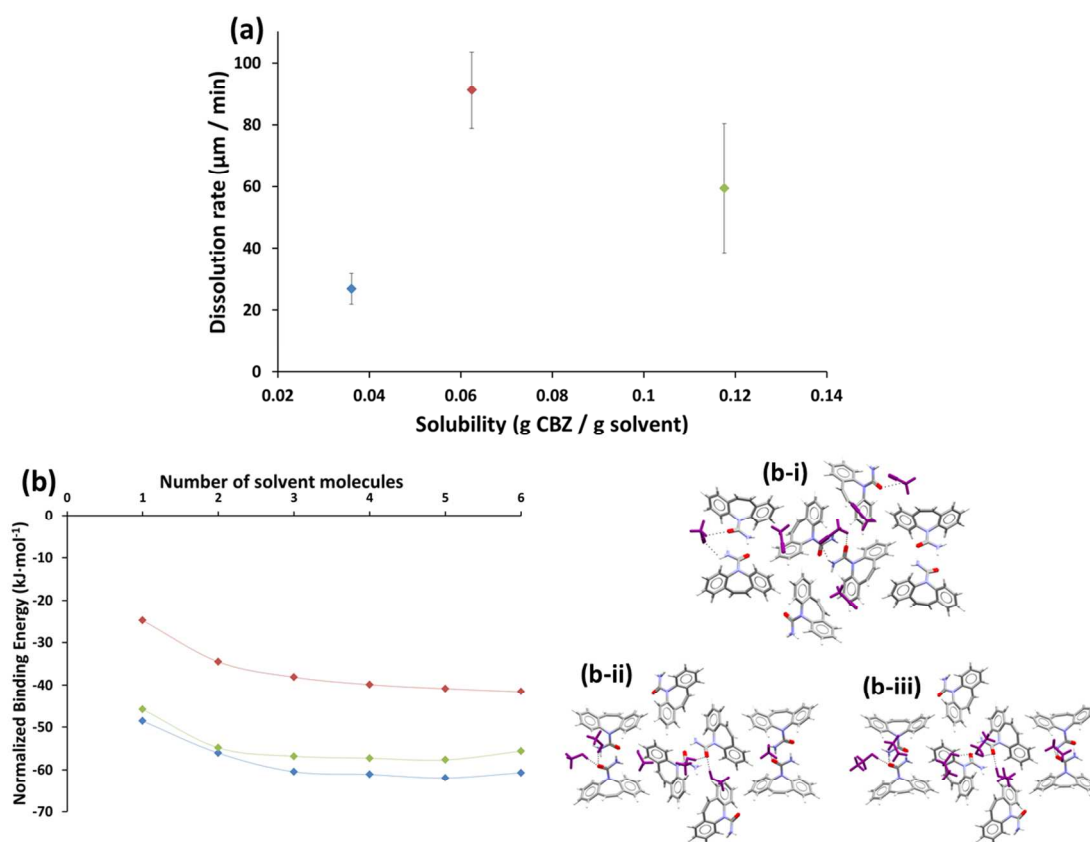


Fig. 4 Experimental dissolution rate of FI crystals in different solvents and computational binding energy of solvent molecules on (100) surface of CBZ FI. (a) Dissolution rate of FI at 20 °C and $\sigma_u = 0.18$ in ethanol \blacklozenge (EtOH) $n=3$, methanol \blacklozenge (MeOH) $n=4$ and acetonitrile \blacklozenge (MeCN) $n=4$, plotted with increasing solubility of FI in each solvent where n is the number of single crystals whose dissolution rate was measured. (b) Normalised binding energy with the number of solvent molecules for ethanol \blacklozenge (EtOH), methanol \blacklozenge (MeOH) and acetonitrile \blacklozenge (MeCN). Low energy packing of six solvent molecules on (100) surface of CBZ FI for (b-i) MeCN, (b-ii) MeOH and (b-iii) EtOH, viewed down the a axis of FI. The solvent molecules are coloured in purple and hydrogen bonds by the dotted lines. CBZ molecules: grey-carbon, white-hydrogen, blue-nitrogen and red-oxygen

As dissolution of FI occurred primarily in the length (a lattice) direction, the dissolution was greatest at the surfaces of FI orthogonal to this direction and the arrangement of the solvent molecules onto the (100) surface of FI were analysed by molecular modelling. The strength of the MeCN binding energy was found to be weaker than that of MeOH and EtOH with little relative change between the solvents with increasing numbers of solvent molecules (Fig. 4b). The MeOH and EtOH molecules were found to bind to the carboxamide groups of CBZ through $-\text{OH}\cdots\text{O}=\text{C}$ hydrogen bond. Upon saturation of all available sites, further solvent \cdots solvent hydrogen bonds were formed and the solvent molecules were clustered around the carboxamide sites on the surface (Fig. 4b-i, 4b-iii). In contrast, MeCN was found to bind in the aromatic pockets of the surface, only binding to the carboxamide group once all these sites are filled (Fig. 4b-ii). The stronger binding solvents EtOH and MeOH exhibited slower dissolution rates relative to the more weakly binding MeCN.

The dissolution of FI was also observed in ethanol with low undersaturation ($\sigma_u = 0.045$ at 20 °C and $\sigma_u = 0.023$ at 30 °C), close to the solubility of FI, more supersaturated with respect to FIII. Unlike the experiments with higher undersaturation with respect to FI ($\sigma_u = 0.18$), under these low undersaturation

conditions, the nucleation and growth of the more stable FIII polymorph occurred (Fig. 5).

At lower undersaturation with respect to FI i.e. higher superaturation with respect to FIII, the dissolving FI crystal underwent dissolution through thinning of the crystal particle (Fig. 5c 5f and 5i). Dissolution occurred through a slow and gradual peeling of the (010) and (001) surfaces which proceeded in the a lattice direction. This was observed in repeat experiments but it was not possible to distinguish whether the thinning occurred more on one face than another due to the relatively small size of these crystal surfaces. Video files showing the dissolution of FI in Fig. 5 are available in the electronic supplementary information. Effectively, the in situ microscopy images in Fig. 5 recorded the solution-mediated polymorphic transformation from FI to FIII. The nucleation and growth of FIII occurred on the surface of the FI crystal particle and was also seen in solution when $\sigma_u = 0.045$ – solution concentration 0.0341 g CBZ / g EtOH. When $\sigma_u = 0.023$ – solution concentration 0.0465 g CBZ / g EtOH nucleation of FIII appeared to occur only on the FI surface. The crystallization of FIII in the solution at low σ_u meant conditions of constant undersaturation for the duration of the experiment were not achievable and any measurable dissolution rate would not be under controlled conditions.

55

Cite this: DOI: 10.1039/c0xx00000x

www.rsc.org/crystengcomm

ARTICLE

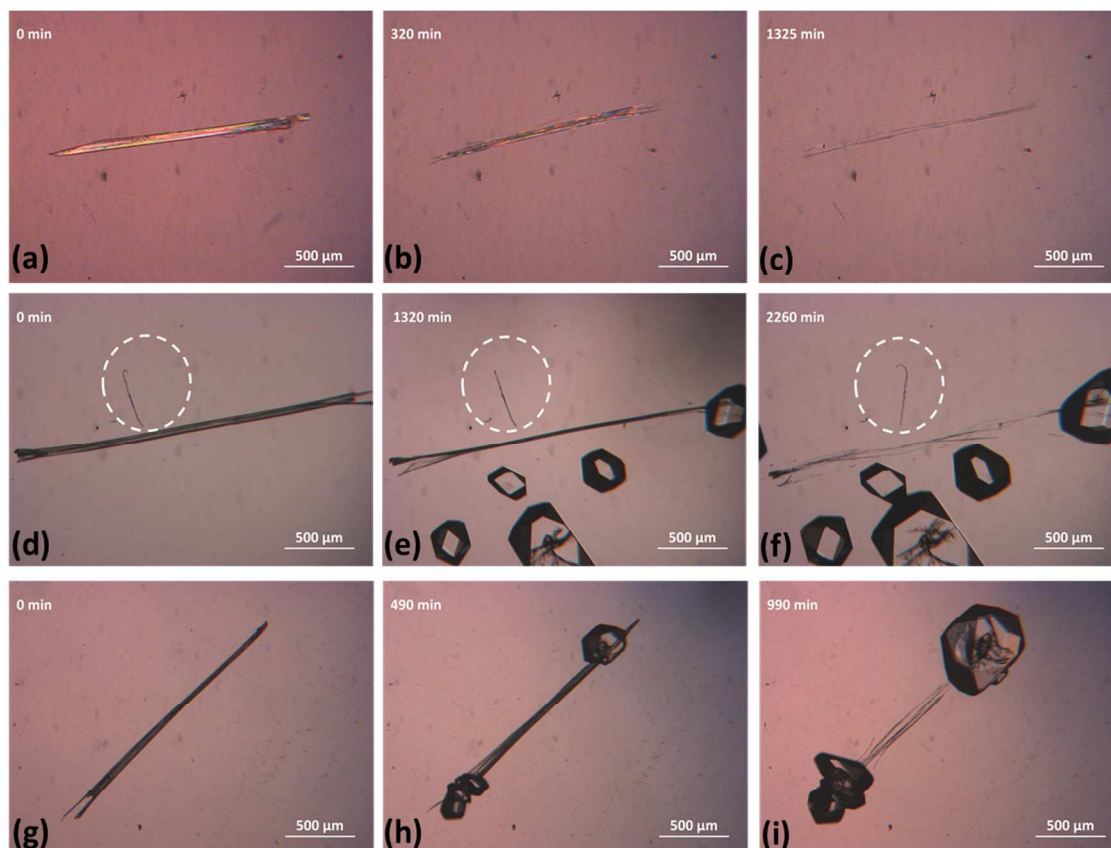


Fig. 5 *In situ* optical microscopy for the dissolution of FI at low undersaturations where the crystallization of the more stable FIII polymorph occurred. (a)–(c) time lapsed images showing the dissolution of FI in ethanol at 20 °C with $\sigma_u = 0.045$ – solution concentration 0.0341 g CBZ / g EtOH. The nucleation and growth of FIII CBZ occurred elsewhere in the holding cell outside of the image. (d)–(f) the dissolution of FI in ethanol at 20 °C with $\sigma_u = 0.045$ – solution concentration 0.0341 g CBZ / g EtOH. A speck of dust, fibre-like, is highlighted in the centre of the images. (g)–(i) the dissolution of FI in ethanol at 30 °C with $\sigma_u = 0.023$ – solution concentration 0.0465 g CBZ / g EtOH.

10 Discussion

The anisotropic dissolution that occurred with $\sigma_u = 0.18$ primarily reduced the length or a lattice direction of the FI crystal, irrespective of the solvent used. The sublimation of FI (Fig. 3e–h) also occurred primarily in the a lattice direction, and this similarity suggests that the dissolution behaviour of FI is likely to be a property of the crystal structure. Similar anisotropic dissolution behaviour has been previously observed in dissolution studies hexamethylmelamine²⁴ where the crystal dissolution behaviour was found to be independent of the solvents used.

Fig. 6 shows the orientation of the CBZ molecules in the FI crystal structure. The molecules are arranged by translation stacking²⁵ along the a lattice direction in the FI crystal structure

(Fig. 6) giving rise to the anisotropic crystal habit of FI. The dissolution and the sublimation, occurring primarily in the crystallographic a lattice direction, will involve detachment of CBZ molecules from the surfaces at either end of the stacked CBZ molecules. Due to the stacking arrangement of CBZ molecules in the FI crystal structure, the CBZ molecules exposed at the exterior ends will have fewer intermolecular CBZ•••CBZ bonding interactions compared to the other CBZ molecules in the crystal structure. This will increase the probability of these CBZ molecules at the (100) end faces detaching from of the needle-like FI crystal structure relative to the CBZ molecules on the other (010) and (001) side faces. This provides a likely explanation for the observation that dissolution and sublimation occurred primarily in the length (a lattice) direction of FI at relatively high undersaturations.

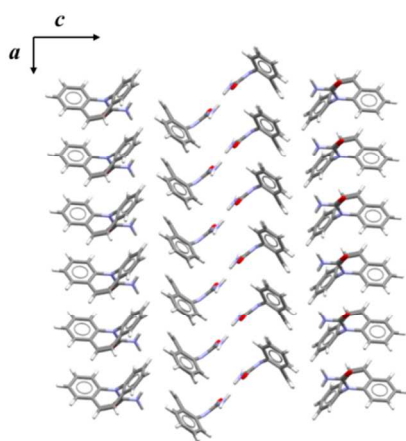


Fig. 6 The relative orientation of CBZ molecules in the FI crystal structure viewed parallel to the crystallographic *a*-axis. For clarity the hydrogen bonded dimer pairs of CBZ are not shown. Colours: grey-carbon, white-hydrogen, blue-nitrogen and red-oxygen

The order of the linear dissolution rates for FI in each of the solvents at a constant driving force was $\text{MeCN} \geq \text{MeOH} > \text{EtOH}$ and did not correlate with the solubility in the solvents (Fig. 4a). The ability of CBZ molecules to detach from the crystal structure of FI and the different solvents to solvate the detached CBZ molecules is likely influenced by parameters relating directly to the solvent. Table 2 summarises some of these parameters.

The cohesive pressure provides a measure of the total strength of the solvent•••solvent interaction.²⁶ The cohesive pressure for each solvent used to dissolve FI is given in Table 2. MeCN has the lowest cohesive pressure and this indicates that the MeCN•••MeCN interactions will be more easily disrupted relative to either MeOH or EtOH. This is likely to facilitate the solvation of CBZ molecules in MeCN once detached from the FI crystal structure more than MeOH or EtOH. However, the cohesive pressure alone does not account for the observed order of the dissolution rates in the solvents.

Table 2 Solvent parameters likely to influence the detachment and solvation of CBZ molecules for each of the solvents used in the dissolution of FI.

Solvent	Average linear dissolution rate ($\mu\text{m}/\text{min}$)	Cohesive pressure ^a ($\text{J}\cdot\text{cm}^{-3}$)	Viscosity ^b ($\text{mPa}\cdot\text{s}$)	Binding energy with (100) surface of FI ^c ($\text{kJ}\cdot\text{mol}^{-1}$)
Ethanol (EtOH)	26.8	676	1.074	-60
Methanol (MeOH)	59.4	858	0.544	-55
Acetonitrile (MeCN)	91.2	581	0.306	-41

^a Data from reference 25. ^b Data from reference 20. ^c Normalised energy of binding for six solvent molecules.

The viscosity of a solvent is inversely proportional to the diffusion of a particle or molecule within that solvent,²⁷ thus a solvent with lower viscosity would be expected to permit faster diffusion of dissolved CBZ molecules. The order of the dissolution rates in each of the solvents is inversely correlated to

the viscosity in each of the solvents (Table 2). This correlation may indicate that the dissolution rate of FI is dependent on the ability of CBZ molecules to diffuse from the dissolving surface of FI. This is not entirely unexpected given that the dissolution experiments were performed in a quiescent solution.

Computational modelling was used to assess the binding interaction of solvent molecules at the dissolving (100) surface of FI. The normalised binding interaction of solvent molecules to the (100) surface of FI from Fig. 4b is reported in Table 2. The order of the linear dissolution rates at $\sigma_u = 0.18$ in each solvent is also inversely correlated to the binding energy of the solvent molecules with the (100) surface of FI. It is well-recognised that specific additives can stabilise etch pits or generate a specific morphology by binding strongly to specific crystallographic faces during dissolution, making the rate at which those faces dissolve, slower in the presence of such strongly binding additives.^{5, 9, 28} Both MeOH and EtOH molecules gave similar, relatively high binding energy with the (100) surface of FI compared to acetonitrile. The higher binding energy of EtOH and MeOH may increase the probability of stabilising and or slowing the detachment of CBZ molecules from the (100) surface of FI in a similar way that additives stabilise the faces to which they can strongly bind. The weaker binding energy seen for MeCN may facilitate a relative increase in the exchange of acetonitrile solvent molecules with the CBZ molecules on the (100) surface of FI which may encourage faster detachment and solvation of CBZ molecules from the surface of FI.

The dissolution at low initial undersaturations $\sigma_u = 0.045$ (Fig. 5) proceeded in the *a* lattice direction of FI but resulted in the gradual peeling of the (010) and (001) surfaces. This was different to the dissolution of FI that occurred at a higher undersaturation (Fig. 3 – no crystallization of FIII) where the dissolution distinctly decreased the length of the FI crystal. This probably reflects a slower propensity to generate initiation points for dissolution on the (100) face of FI in lower undersaturation conditions. It is well known that dissolution at low σ_u is typically characterised by retreating steps which can be initiated at defects or dislocation sites on the crystal surface.²⁹ Dissolution can begin at a defect initiation point such that an entire line of stacked CBZ molecules may retreat directly in line with an initiation point in the *a* direction before a another initiation point is generated. Such a process may lead to the peeling of the (010) and (001) surfaces as observed. At higher σ_u , multiple initiation points occurring on the (100) face of FI could result in the overall decrease in the length of the FI crystal and such a mechanism is typically expected at higher undersaturations.^{4, 29} This represents a difference in surface dissolution mechanism at low σ_u relative to that at high σ_u .

The transformation from FI to FIII only occurs at low σ_u . In a previous study, it has been shown that the stable FIII can nucleate and grow on the surfaces of FI parallel to the *a* direction during the transformation.³⁰ Furthermore, the dissolution of FI also favours the nucleation of FIII at the surface of FI.³⁰ Specifically it is hypothesised that FI dissolution exposes the dibenzazepine portion of CBZ molecules at the surface of FI. These dibenzazepine groups are known to stack in FI but in the FIII

structure they pack in an inverted manner.²⁵ The increased presence of such groups due to the dissolution of the stacked CBZ molecules in FI (at low σ_u) may facilitate the formation of the inverted packing of CBZ molecules, characteristic of FIII, to be adopted between molecules at the surface of FI and CBZ molecules in the solution, leading to the nucleation of FIII on the side faces of the FI needle-like crystal (Fig. 5 d-f, 5 g-i). Dissolution at high σ_u does not preserve these side surfaces in the same way but rather dissolves them as the length of the needle-like FI crystal decreases (Fig. 3 a-c). Subsequently, at high σ_u the nucleation of stable FIII does not occur. This identifies the potential role of different surface dissolution mechanisms in the solution-mediated transformation from FI to FIII CBZ and is a worthy consideration for the analysis of SMPT in general.

15 Conclusions

The sublimation and dissolution of FI occurs in the length (*a* lattice) direction of the crystal particle regardless of the solvents used. This can be rationalised in terms of the stacking orientation of the CBZ molecules relative to the *a* lattice direction of the crystal structure. The order of the dissolution rate for FI in the different solvents was MeCN \geq MeOH > EtOH and does not correlate with the solubility in the solvents. The order of the dissolution rates in each of the solvents is inversely correlated with the viscosity and the binding energy of the solvents with the (100) surface of FI in each of the solvents. This suggests that the rate determining step for the dissolution may be either the diffusion or the detachment of CBZ molecules from the surface of FI. The change in dissolution mechanism at low undersaturations affects the surface of FI crystals differently compared to dissolution at high undersaturation. This has direct implications for the solution-mediated transformation from FI to FIII considering that this transformation occurs at concentrations that represent very low undersaturations and that FIII can nucleate and grow on the surface of FI.

35 Acknowledgements

The authors thank Nicole Walshe and Prof. Pat McArdle for single crystal X-ray diffraction, the Science Foundation of Ireland (SFI) for the Short Term Travel Fellowship supplement which enabled the in situ microscopy work to be carried out in the laboratory of Prof. Stéphane Veesler at the Centre Interdisciplinaire de Nanosciences de Marseille, France. The work is supported by the Solid State Pharmaceutical Cluster and the SFI under Grant 07/SRC/B1158.

45 Notes and references

- ^a *Synthesis and Solid State Pharmaceutical Centre, Materials and Surface Science Institute, Department of Chemical and Environmental Sciences, University of Limerick, Limerick, Ireland. Fax: +353 61 213529; Tel: +353 61 233754; E-mail: colin.seaton@ul.ie, ake.rasmuson@ul.ie, kieran.hodnett@ul.ie.*
- ^b *MIT-Novartis Center for Continuous Manufacture, Department of Chemical Engineering, Massachusetts Institute of Technology, 77 Massachusetts Ave, Cambridge, MA 02138. Tel: +1 617 324 4525; E-mail: *omahonym@mit.edu.*
- ^c *CINaM-CNRS, Campus de Luminy, Case 913, 13288 Marseille Cedex, France. Tel: +33(0)4 91 17 28 00; E-mail: veesler@cinam.univ-mrs.fr*

† Electronic Supplementary Information (ESI) available: video files given for the dissolution of FI in Fig. 3a-d, Fig. 5a-c, Fig. 5d-f, Fig. 5g-i and the sublimation in Fig. 3e-h. Time lapsed images and dissolution rates for the sublimation of FI at 165°C and the dissolution of FI in MeCN and MeOH are also given in addition to their video files. See DOI: 10.1039/b000000x/

1. A. Putnis, *Mineralogical Magazine*, 2002, **66**, 689-708.
2. A. Saleemi, C. Rielly and Z. K. Nagy, *CrystEngComm*, 2012, **14**, 2196-2203.
3. P. T. Cardew and R. J. Davey, *Proceedings of the Royal Society of London. Series A, Mathematical and Physical Sciences*, 1985, **398**, 415-428.
4. P. M. Dove, N. Han and J. J. De Yoreo, *Proceedings of the National Academy of Sciences of the United States of America*, 2005, **102**, 15357-15362.
5. L. J. W. Shimon, M. Lahav and L. Leiserowitz, *Journal of the American Chemical Society*, 1985, **107**, 3375-3377.
6. M. Lahav and L. Leiserowitz, *Journal of Physics D: Applied Physics*, 1993, **26**, B22.
7. R. Davey, W. Fila and J. Garside, *Journal of Crystal Growth*, 1986, **79**, 607-613.
8. R. J. Davey, N. Blagden, G. D. Potts and R. Docherty, *Journal of the American Chemical Society*, 1997, **119**, 1767-1772.
9. C. Wu, X. Wang, K. Zhao, M. Cao, H. Xu, D. Xia and J. R. Lu, *Crystal Growth & Design*, 2011, **11**, 3153-3162.
10. R. C. Snyder, S. Veesler and M. F. Doherty, *Crystal Growth & Design*, 2008, **8**, 1100-1101.
11. A. A. Noyes and W. R. Whitney, *Journal of the American Chemical Society*, 1897, **19**, 930-934.
12. G. L. Amidon, H. Lennernäs, V. P. Shah and J. R. Crison, *Pharmaceutical Research*, 1995, **12**, 413-420.
13. A. Dokoumetzidis and P. Macheras, *International Journal of Pharmaceutics*, 2006, **321**, 1-11.
14. R. Hilfiker, F. Blatter and M. v. Raumer, in *Polymorphism*, Wiley-VCH Verlag GmbH & Co. KGaA, 2006, pp. 1-19.
15. M. O'Mahony, A. Maher, D. M. Croker, Å. C. Rasmuson and B. K. Hodnett, *Crystal Growth & Design*, 2012, **12**, 1925-1932.
16. S. Veesler, L. Lafferrère, E. Garcia and C. Hoff, *Organic Process Research & Development*, 2003, **7**, 983-989.
17. S. Veesler, N. Fertè, M.-S. Costes, M. Czjzek and J.-P. Astier, *Crystal Growth & Design*, 2004, **4**, 1137-1141.
18. K. T. No, O. Y. Kwon, S. Y. Kim, K. H. Cho, C. N. Yoon, Y. K. Kang, K. D. Gibson, M. S. Jhon and H. A. Scheraga, *The Journal of Physical Chemistry*, 1995, **99**, 13019-13027.
19. F. Neese, *Wiley Interdisciplinary Reviews: Computational Molecular Science*, 2012, **2**, 73-78.
20. R. Storn and K. Price, *Journal of Global Optimization*, 1997, **11**, 341-359.
21. A. L. Grzesiak, M. Lang, K. Kim and A. J. Matzger, *Journal of Pharmaceutical Sciences*, 2003, **92**, 2260-2271.
22. M. A. O'Mahony, D. M. Croker, Å. C. Rasmuson, S. Veesler and B. K. Hodnett, *Organic Process Research & Development*, 2012, **17**, 512-518.
23. J. Miller, N. Rodriguez-Hornedo, A. Blackburn, D. Macikenas and B. Collman, in *Solvent Systems and Their Selection in*

- Pharmaceutics and Biopharmaceutics*, eds. P. Augustijns and M. E. Brewster, Springer New York, 2007, pp. 53-109.
24. G. A. Rodley, H.-K. Chan and I. Gonda, *International Journal of Pharmaceutics*, 1993, **95**, 143-151.
- 5 25. S. L. Childs, P. A. Wood, N. Rodriguez-Hornedo, L. S. Reddy and K. I. Hardcastle, *Crystal Growth & Design*, 2009, **9**, 1869–1888.
26. C. Reichardt and T. Welton, in *Solvents and Solvent Effects in Organic Chemistry*, Wiley-VCH Verlag GmbH & Co. KGaA, 2010, pp. 65-106.
- 10 27. A. Einstein, *Zeitschrift für Elektrochemie und angewandte physikalische Chemie*, 1908, **14**, 235-239.
28. S. Guo, M. D. Ward and J. A. Wesson, *Langmuir*, 2002, **18**, 4284-4291.
29. P. M. Dove and N. Han, *AIP Conference Proceedings*, 2007, **916**, 215-234.
- 15 30. M. O'Mahony, C. C. Seaton, D. M. Croker, S. Veessler, Å. C. Rasmuson and B. K. Hodnett, *Crystal Growth & Design*, 2013, **13**, 1861-1871.

20

Investigating the Dissolution of the Metastable Triclinic Polymorph of Carbamazepine using *in situ* Microscopy

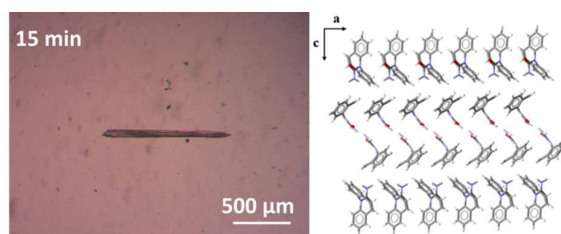
M. O'Mahony,^{*a, b} C. C. Seaton,^a D.M. Croker,^a S.Veesler,^c Å. C. Rasmuson^a and B. K. Hodnett^a

^a Synthesis and Solid State Pharmaceutical Centre, Materials and Surface Science Institute, Department of Chemical and Environmental Sciences, University of Limerick, Limerick, Ireland. Fax: +353 61 213529; Tel: +353 61 233754; E-mail: colin.seaton@ul.ie, ake.rasmuson@ul.ie, kieran.hodnett@ul.ie.

^b MIT-Novartis Center for Continuous Manufacture, Department of Chemical Engineering, Massachusetts Institute of Technology, 77 Massachusetts Ave, Cambridge, MA 02138. Tel: +1 617 324 4525; E-mail: omahonym@mit.edu.

^c CINaM-CNRS, Campus de Luminy, Case 913, 13288 Marseille Cedex, France. Tel: +33(0)4 91 17 28 00; E-mail: veesler@cinam.univ-mrs.fr

TOC



Despite the tendency to undergo solution-mediated transformation, the dissolution behaviour of the metastable FI polymorph of carbamazepine was studied. The results are rationalized on the basis of its crystal structure.